X chromosome protects against bladder cancer in females via a KDM6A-dependent epigenetic mechanism

CANCER

X chromosome protects against bladder cancer in females via a *KDM6A*-dependent epigenetic mechanism

Satoshi Kaneko and Xue Li*

Men are much more likely than women to develop bladder cancer (BCa), but the underlying cause of this gender disparity remains poorly defined. Using sex-reversed mice, we show that the sex chromosome complement is an independent cause and, moreover, amplifies the biasing effects of sex hormones. We also show that the X-linked lysine demethylase 6A (*KDM6A*) is a sexually dimorphic gene. Wild-type but not catalytically dead *KDM6A* confers sustained tumor suppressor activity in vitro. Knockout of mouse *Kdm6a* reduces expression of *Cdkn1a* and *Perp*, canonical gene targets of the tumor suppressor *p53*. Consistently, loss of *Kdm6a* increases BCa risk in female mice, and mutations or reduced expression of human *KDM6A* predicts poor prognosis of female BCa patients. Collectively, the study reveals that the X chromosome protects against BCa among females via a *KDM6A*-dependent epigenetic mechanism and further suggests that *KDM6A* is a prototypical sex-biasing tumor suppressor with both demethylase-dependent and demethylase-independent activities.

INTRODUCTION

Men are much more likely than women to develop and die from cancer (*1*). However, the male dominance of cancer risk remains poorly understood. Bladder cancer (BCa) is the fourth most common cancer among men, and the incidence rate of BCa is three to five times higher among men than women (*2*). Gender disparity in BCa persists even after the known risk factors, including cigarette smoking, occupational hazards, and urinary tract infection, are taken into consideration (*3*).

Rodents also exhibit sex differences in cancer. For example, when mice are exposed ad libitum to *N*-butyl-*N*-(4-hydroxybutyl)nitrosamine (BBN), a bladder-specific chemical carcinogen, male mice develop and die from BCa significantly sooner than female mice (*4*). The sex difference in BBN-induced BCa is unlikely due to differences in exposure and response to the carcinogen because the BBN-induced DNA mutation rates are the same between sexes (*5*). Castration or androgen receptor gene deletion, however, significantly reduces BBN-induced BCa risk among male mice (*4*, *6*, *7*), indicating that sex hormones, particularly androgens, are major contributors to sex differences in BCa. While the pathogenesis of BBN-induced mouse BCa may not be directly comparable to human BCa, this model nevertheless exhibits similar histopathology (*8*, *9*) and recapitulates the sex disparities of human BCa. Collectively, the sex difference in cancer appears to be an intrinsic biological feature conserved in mouse and human.

In mammals, sex differences primarily stem from the inequality in effects of sex chromosomes (*10*): XY males have one copy each of X and Y chromosomes, while XX females have two copies of the X chromosome. This difference initiates dimorphic gonadal differentiation and results in the differences in effects of sex hormones. Specifically, effects of the Y chromosome result in the development of testis, from which androgens regulate male differentiation and behavior. Likewise, the XX chromosomal complement is linked to ovary differentiation and female sex hormones. Sex chromosomes may have additional sex-biasing effects independent of gonadal differentiation and sex hormones. For example, nearly 23% of human and 5% of mouse X chromosome genes escape X chromosome inactivation (XCI) and are expressed at significantly higher levels in XX cells than in XY cells (*11*–*13*). Together, sex chromosomes and sex hormones may either enhance or compensate each other's biasing effects (*14*). Ultimately, gender disparities in cancer likely result from the combined and independent effects of multiple interrelated sex-biasing factors, including biological, behavioral, and environmental factors.

Independent biasing effects of sex chromosomes and sex hormones are difficult to discern because they are coupled and covary with each other. Possible biasing effects of sex chromosomes on BCa development have yet to be determined. By uncoupling their effects and using mouse models and data from human patients, we provide initial genetic and molecular evidence suggesting that the chromosomal difference (XX versus XY) between sexes is an intrinsic cause of sex difference in BCa via a *KDM6A*-dependent epigenetic mechanism.

Department of Urology and Surgery, Boston Children's Hospital, Harvard Medical School, 300 Longwood Avenue, Boston, MA 02115, USA.
*Corresponding author. Email: sean.li@childrens.harvard.edu

RESULTS

Sex chromosomes play an independent role in the sex differences in BCa

To determine the independent and combined sex-biasing effects of sex chromosomes and sex hormones, we used the sex-reversed or "four core genotypes" (FCG) mice, in which the gonadal sex (testis and ovary) and the genetic sex (XX and XY) are uncoupled (*15*). The FCG mice consist of XX and XY males (XXM and XYM) with testes and XX and XY females (XXF and XYF) with ovaries (Fig. 1A). XXM and XYM mice have comparable blood levels of testosterone, and XXF and XYF mice exhibit similar estrous cycles. All four groups of mice (7 to 8 weeks old) were exposed to BBN in the drinking water to induce BCa formation. Overall survival of the mice was monitored and recorded for 40 weeks (Fig. 1B). Mice that survived at the end of the 40-week regimen were sacrificed and considered as censored (Fig. 1C and fig. S1). Two comparisons were made to determine the independent effects of the sex hormones (XXF versus XXM and XYF versus XYM) and sex chromosomes (XXF versus XYF and XXM versus XYM) (Fig. 1, C and D). Survival of XXF and XYF mice in response to BBN-induced BCa was significantly better than XXM and XYM mice, respectively ($P < 0.0001$ in both comparisons), supporting the notion that effects of sex hormones contribute significantly to sex differences in BCa. Overall survival of XXF and XXM mice was also significantly better than of XYF and XYM mice ($P = 0.025$ and 0.0017), respectively. Therefore, sex chromosomes play a previously unknown sex-biasing role that is independent of sex hormones during BCa development.

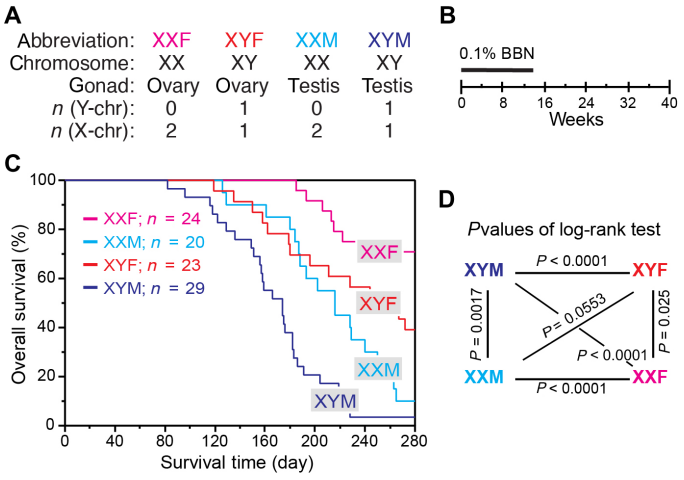

Fig. 1. Sex chromosomes play an important and independent role in sex difference in BCa. (**A**) Schematic diagram of the sex-reversed or FCG mice. (**B**) Outline of the BBN-induced BCa regimen. BBN (0.1%) is supplied to mice (7 to 8 weeks old) in drinking water for 14 weeks. Mice are monitored daily for death or moribundity. (**C** and **D**) Kaplan-Meier analysis of overall survival of the FCG mice after BBN exposure (C) and *P* values are shown in (D) (log-rank test). Mice that survive the 40-week regimen are considered as censored.

Sex chromosomes amplify the biasing effects of sex hormones

To determine the significance of sex chromosomes and sex hormones in BCa risk relative to each other, we compared the overall survival of the FCG XX mice to that of XY mice and the overall survival of mice with testes to that of mice with ovaries. Regardless of the gonadal types, the likelihood of XY mice developing and dying from BBN-induced BCa was significantly higher than of the XX mice ($P = 0.0007$). The hazard ratio (HR) between XY and XX mice was 2.549 with a 95% confidence interval (CI) between 1.55 and 4.28 (Table 1). Mice with testes were much more susceptible to BCa with an HR of 4.714 ($P < 0.0001$). The combined effect of sex chromosomes and sex hormones (that is, XXF versus XYM) markedly increased the HR to 12.390 (95% CI, 5.54 to 31.63), which is equivalent to the product of HRs of sex chromosomes and sex hormones. Together, these findings suggest that sex chromosomes and sex hormones contribute independently to sex bias and, together, function synergistically to amplify sex differences in BCa.

X-linked *Kdm6a* is a sexually dimorphic gene that acts as a demethylase-dependent and demethylase-independent tumor suppressor

Conceptually, the biasing effects of sex chromosomes could stem from the possible oncogenic activity of a Y chromosome and/or tumor suppressor activity of an X chromosome. The Y chromosome is frequently lost in BCa cells (*16*), and its loss increases cancer risk (*17*). Hence, it is highly unlikely that the Y chromosome plays an overall oncogenic role to increase BCa risk among men. Therefore, we considered a tumor suppressor role of the X chromosome, focusing on the sexually dimorphic XCI escape genes. The number of XCI escape genes differs among different tissue types and species (*11*–*13*). To identify bladder urothelium–enriched XCI escape genes, we performed RNA sequencing (RNA-seq) analysis of urothelium from FCG mice and identified X-linked lysine demethylase 6A (*Kdm6a*) as a top differentially expressed gene (DEG) between XX and XY urothelial cells (Fig. 2A). Quantitative analysis confirmed that the sexually biased expression of *Kdm6a* is independent of gonadal types (Fig. 2B).

Table 1. Independent and combined biasing effects of the sex chromosomes and gonadal hormones in BCa. The HR is determined using the Cox proportional hazard model. Chro, sex chromosomes; *n*, mouse numbers; O, ovary; T, testis.

	n	HR	*P*	95% CI
Chro (XY vs. XX)	(52, 44)	2.549	0.0002	1.55–4.28
Gonad (T vs. O)	(49, 47)	4.714	<0.0001	2.77–8.28
Combination	(29, 24)	12.39	<0.0001	5.54–31.63

Depending on the molecular context, human *KDM6A* has been reported as an oncogene in breast cancer (*18*) while playing a tumor suppressor role in T cell acute lymphoblastic leukemia (*19*–*21*). To determine the possible role of *KDM6A* in BCa cells, we used human UM-UC-13, which lacks endogenous *KDM6A* because of a frameshift mutation (*22*), and mouse MB49, which shares similarities with human BCa, including cell surface markers, sensitivity to apoptosis, and immunological profile (*23*). Stable expression of human *KDM6A* significantly inhibited proliferation of MB49 cells (Fig. 2C). The catalytically dead *KDM6A* mutant (H1146A/E1148A, Mut) (*24*, *25*) also inhibited MB49 cell proliferation, albeit with lower efficacy than wild-type *KDM6A*. Both UM-UC-13 and MB49 parental cells formed colonies in soft agar assay, demonstrating anchorage-independent growth in these tumor cell lines (Fig. 2D and fig. S2, A to C). Expression of *KDM6A* significantly reduced colony size and number, with wild-type *KDM6A* being much more effective than the catalytically dead mutant (Fig. 2D).

To determine whether the intrinsic demethylase activity of *KDM6A* could confer a sustained effect, we used a doxycycline-inducible system to express *KDM6A* transiently in UM-UC-13 cells (fig. S2D). Parental cells without *KDM6A* and cells that expressed *KDM6A* persistently were used as negative and positive controls, respectively. Expression of both wild-type and mutant *KDM6A* was observed after doxycycline induction but became almost undetectable 3 days after doxycycline withdrawal (Fig. 2, E and F). Wild-type *KDM6A*, regardless of transient or sustained expression, significantly inhibited cell proliferation (Fig. 2G). However, transient expression of the mutant had no detectable effect despite its ability to significantly repress cell proliferation when persistently expressed (Fig. 2H). Collectively, these observations suggest that *KDM6A* acts as a tumor suppressor in vitro through both demethylase-dependent and demethylase-independent mechanisms. In addition, wild-type but not mutant *KDM6A* confers sustained tumor suppressor activity.

Conditional knockout of mouse *Kdm6a* increases BCa risk among females in vivo

To determine whether *Kdm6a* functions as a tumor suppressor in vivo, we crossed mice with a conditional allele of *Kdm6a* (*24*) with a urothelium-specific *Cre* driver, *Upk2-Cre* (*26*). The resulting *Kdm6a* conditional knockout (cKO) mice were viable and fertile with no apparent phenotype. A total of 85.7% of *Kdm6a* cKO females died within the 40-week BBN-induced BCa regimen, and all of them (100%) developed macroscopically detectable BCa (Fig. 3 and fig. S3). This differed sharply with wild-type females (that is, XXF), of which 30.4% died and 50% had detectable BCa (fig. S1). Overall survival of *Kdm6a* cKO females was worse than

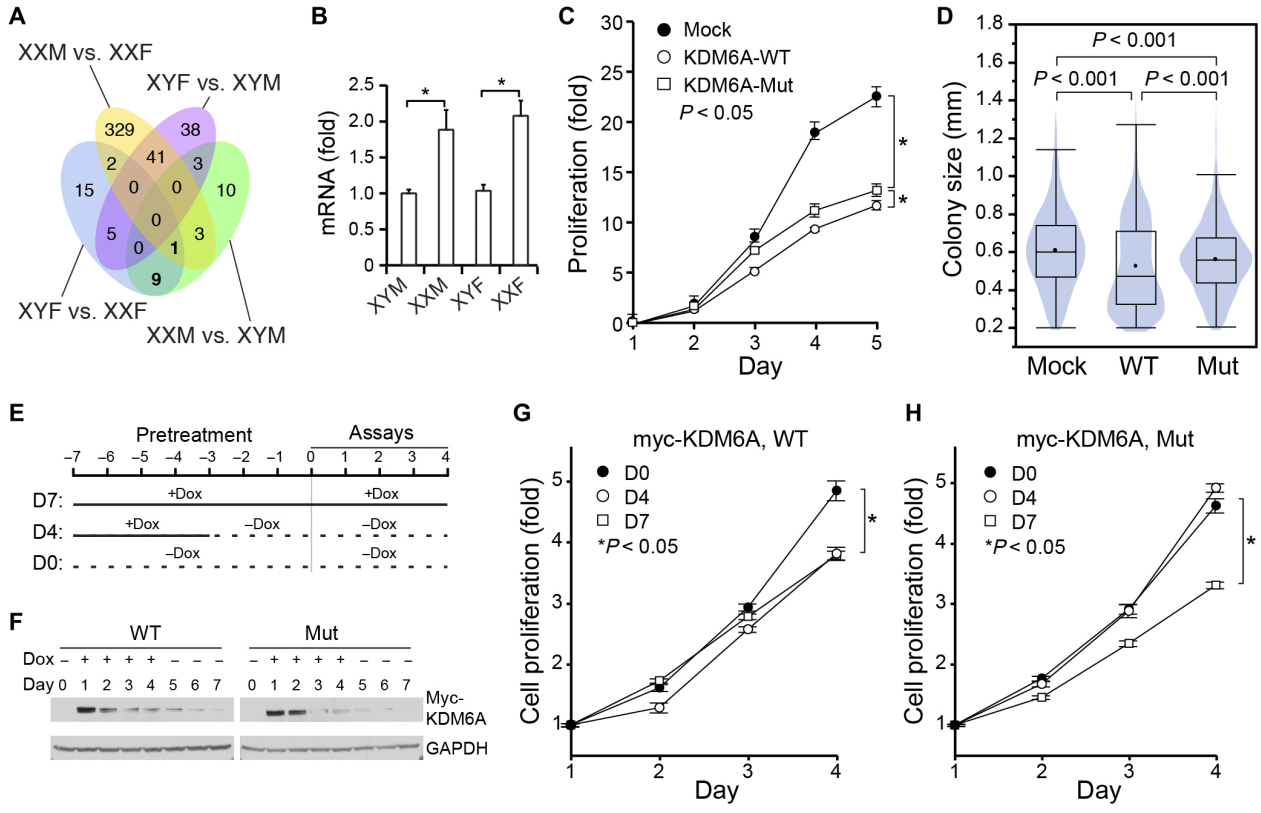

Fig. 2. *KDM6A* functions as a demethylase-dependent and demethylase-independent tumor suppressor of BCa. (**A**) Venn diagram of the DEGs identified by RNA-seq analysis of bladder urothelium. (**B**) Quantitative *Kdm6a* expression levels [quantitative reverse transcription polymerase chain reaction (qRT-PCR)] in bladder urothelium. Glyceraldehyde-3-phosphate dehydrogenase (GAPDH) is used as an internal control. $n = 3$, Student's t test. (**C** and **D**) Cell proliferation rate (C) and anchorage-independent growth in soft agar assay (D) are measured and compared between MB49 BCa cells that express either wild-type (WT) or the catalytically dead (Mut) *KDM6A*. Mock, parental cells with vector control; *$P < 0.05$, Student's t test. (**E** and **F**) Schematics of the doxycycline (Dox)–inducible strategy (E) to express transiently the myc-tagged wild-type (WT) or mutant (Mut) *KDM6A* (myc-*KDM6A*) in UM-UC-13 cells. Cell lysates were immunoblotted using Myc and GAPDH-specific antibodies (F). (**G** and **H**) Cell proliferation assays. D0, without Dox; D4, transient Dox induction for 4 days; D7, persistent Dox induction for 7 days; *$P < 0.05$, Student's t test.

control females ($P = 0.0048$; Fig. 3A). Mutant males without *Kdm6a*, however, displayed no significant difference in survival or tumor burden from control males ($P = 0.2732$). This is likely due to the compensatory effects of *Uty* (*24*), a paralog of *Kdm6a* on the Y chromosome. Alternatively, *Kdm6a* may function differently between sexes. While the overall survival of *Kdm6a* cKO males was worse than the mutant females ($P = 0.0261$), the HR of wild-type mice between sexes was much higher than that of the mutants without *Kdm6a*, at 12.390 versus 2.349, respectively (Table 1 and table S1). Hence, urothelium-specific deletion of *Kdm6a* resulted in more than a fivefold reduction of sex differences in BCa, suggesting that X-linked tumor suppressor *Kdm6a* plays a major role in the sex-biasing effects of X chromosome in BCa.

Kdm6a promotes expression of *Cdkn1a* and *Perp*, the canonical *p53* gene targets

To identify *Kdm6a*-dependent gene targets that are responsible for the tumor suppression activity in bladder urothelium, we performed RNA-seq analysis to compare *Kdm6a* homozygous cKO females and sex-matched wild-type controls. Among the DEGs, 391 were significantly down-regulated, while 156 were up-regulated in the *Kdm6a* mutants [adjusted P (P_{adj}) < 0.05; Fig. 3B]. Ingenuity Pathway Analysis of the DEGs predicted that the *p53* tumor suppressor pathway and the extracellular signal–regulated kinase/mitogen-activated protein kinase (ERK/MAPK) signaling pathway are among the top three most affected canonical pathways. Among the canonical *p53* downstream gene targets (*27*), *Cdkn1a* and *Perp*, which induce cell cycle arrest and apoptosis, respectively, were reduced significantly in *Kdm6a* cKO mutants (Fig. 3C).

Complementary to the gene deletion approach, we examined whether expression of human *KDM6A* is sufficient to activate endogenous *CDKN1A* and *PERP* gene expression in UM-UC-13 cells (Fig. 3, D and E). Wild-type *KDM6A* significantly induced the expression of both *CDKN1A* and *PERP*, while the catalytically dead *KDM6A* mutant only induced the expression of *PERP* but not of *CDKN1A*. Chromatin immunoprecipitation (ChIP) further revealed that expression of both wild-type and mutant *KDM6A* resulted in the significant reduction of histone H3 Lys^{27} trimethylation (H3K27me3), an epigenetic transcription-repressive mark, at the *CDKN1A* and *PERP* loci (Fig. 3, F and G). The transcription activation mark H3K4me3, however, was increased at the *PERP* locus but was reduced at the *CDKN1A* when the effects of the mutant were compared to wild-type *KDM6A*.

Kdm6a demethylase function opposes polycomb repressive complex 2 (PRC2) activity by removing the methyl groups from H3K27me3. We reasoned that *Kdm6a* demethylase–dependent gene targets are also regulated by PRC2. *Eed* is an obligatory component of PRC2. We have reported that urothelium-specific cKO of *Eed* completely abolishes PRC2 activity (*26*). We found that *Cdkn1a* was significantly up-regulated

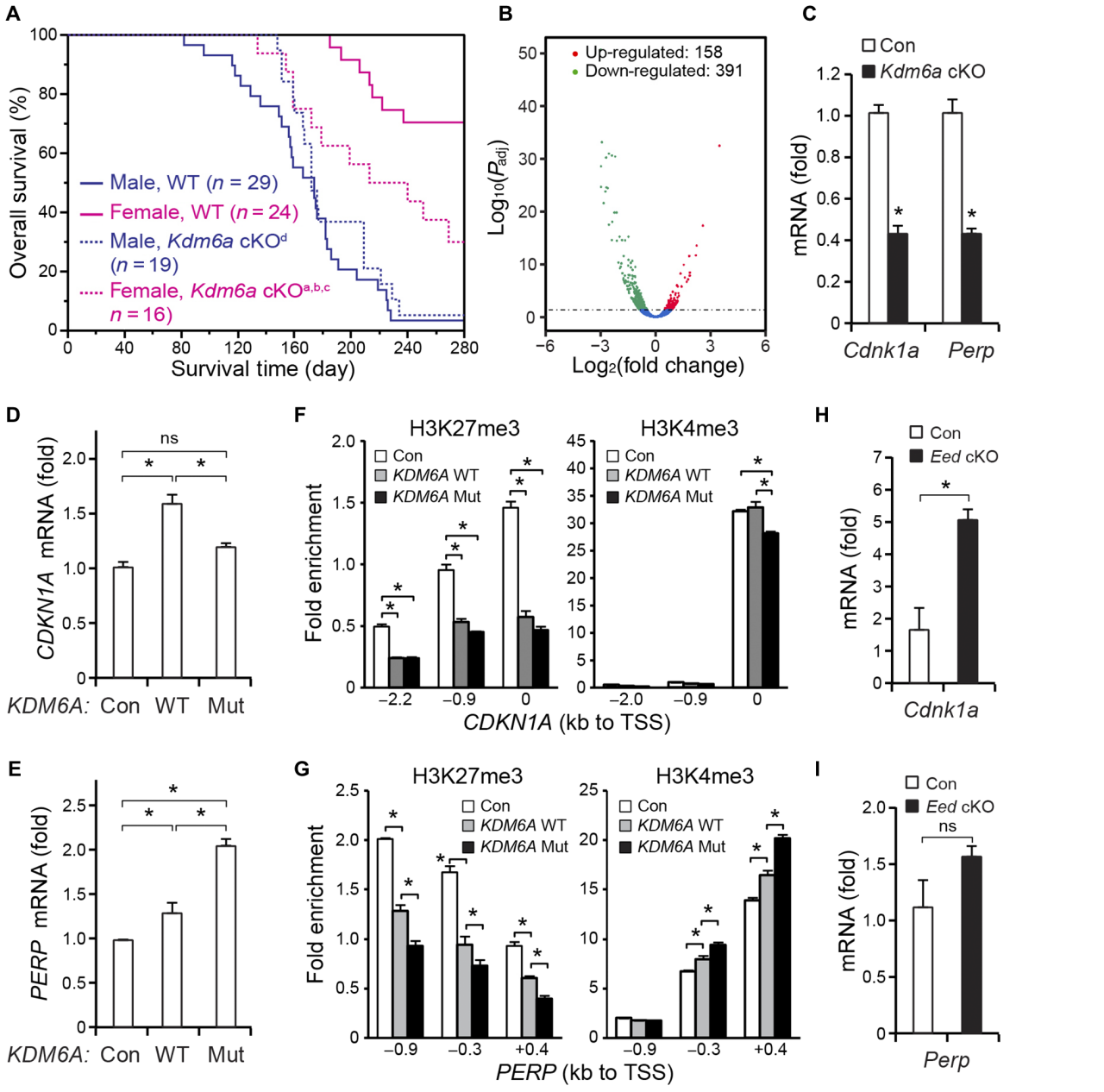

Fig. 3. Knockout of *Kdm6a* significantly increases BCa risk among female mice. (**A**) Kaplan-Meier analysis of overall survival of control and *Kdm6a* cKO mice under the BBN-induced BCa regimen. [a]$P = 0.0048$, XXF *Kdm6a* cKO versus XXF WT; [b]$P = 0.0025$, XXF *Kdm6a* cKO versus XYM WT; [c]$P = 0.0261$, XXF *Kdm6a* cKO versus XYM *Kdm6a* cKO; [d]$P = 0.2732$, XYM *Kdm6a* cKO versus XYM WT; log-rank test. (**B**) Volcano plot of the DEGs of bladder urothelium between wild-type and homozygous *Kdm6a* cKO females ($n = 2$; $P_{adj} < 0.05$). (**C**) qRT-PCR analysis of the candidate *Kdm6a* gene targets *Cdnk1a* and *Perp* in bladder urothelium of *Kdm6a* cKO mice. (**D** and **E**) qRT-PCR analysis of endogenous *CDKN1A* (D) and *PERP* (E) gene expression in UM-UC-13 cells that express either wild-type or catalytically dead *KDM6A*. *$P < 0.05$; ns, not significant, Student's *t* test. (**F** and **G**) Chromatin immunoprecipitation (ChIP) and quantitative PCR (qPCR) assays of UM-UC-13 cells shown in (D) and (E) using H3K27me3- and H3K4me4-specific antibodies. Location of the qPCR primer relative to the transcription start site (TSS) is indicated. *$P < 0.01$, Student's *t* test. (**H** and **I**) qRT-PCR analysis of *Cdnk1a* (H) and *Perp* (I) gene expression in bladder urothelium of *Eed* cKO mice. GAPDH is used as an internal control. $n = 3$, Student's *t* test.

in the bladder urothelium of *Eed* cKO mice (Fig. 3H). Expression of *Perp*, however, was not affected in *Eed* mutants (Fig. 3I), consistent with the notion that its expression does not depend on *Kdm6a* demethylase activity. Collectively, these findings suggest that *Kdm6a* promotes *p53* tumor suppressor activity by enhancing the expression of *p53* gene targets, including *Cdkn1a* and *Perp*, via demethylase-dependent and demethylase-independent mechanisms, respectively.

Human *KDM6A* is closely linked to progression and prognosis of female BCa patients

To determine possible sex-biasing effects of *KDM6A* in human BCa, we examined patients' genomic and clinical data available from The Cancer Genome Atlas (TCGA) project (*28*–*31*). Transcriptomic analysis of BCa samples from 412 patients (304 males and 108 females) showed that *KDM6A* expression was significantly higher in females than in males

(Fig. 4A). Reduced *KDM6A* expression correlated tightly with BCa progression to advanced stages (Fig. 4B). Mutations of *KDM6A* associated tightly with reduced disease-free survival of BCa patients (Fig. 4C). Reduced *KDM6A* expression also predicted poor disease-free survival of BCa patients (Fig. 4D). Consistent with the observations from *Kdm6a* cKO mice (Fig. 3A), these correlations were only observed in females but not in males. Collectively, these findings suggest that human *KDM6A* mutations and reduced expression predict poor prognosis of female BCa patients.

Female-biased *KDM6A* expression was also observed in other cancers, including colorectal adenocarcinoma, head and neck squamous cell carcinoma, kidney renal clear cell carcinoma, liver hepatocellular carcinoma, lung adenocarcinoma, and pancreatic adenocarcinoma (fig. S4). Reduced *KDM6A* expression correlated tightly with poor overall survival of patients with BCa and renal clear cell carcinoma but not with other cancer types examined (fig. S5), suggesting that *KDM6A* is a tissue-specific tumor suppressor. In addition to *KDM6A*, we have also analyzed 15 candidate X-linked genes that have been reported to escape XCI in both human and mouse (*11*–*13*). Somatic mutations of these genes in human BCa ranged from 0% for *XIST* to 24% for *KDM6A* (fig. S6). Among all these candidates, only a subset of seven genes (*KDM6A*, *DDX3X*, *EIF2S3*, *JPX*, *KDM5C*, *MID1*, and *XIST*) displayed female-biased expression in BCa (fig. S7), consistent with the notion that the XCI status differs among tissues. Two of the 16 candidates, *KDM6A* and *DDX3X*, closely associated with overall survival of BCa patients (fig. S8). Together, these clinical observations confirm that the sex-biasing effects of the X chromosome are mediated, in part, by XCI escape genes, including *KDM6A*.

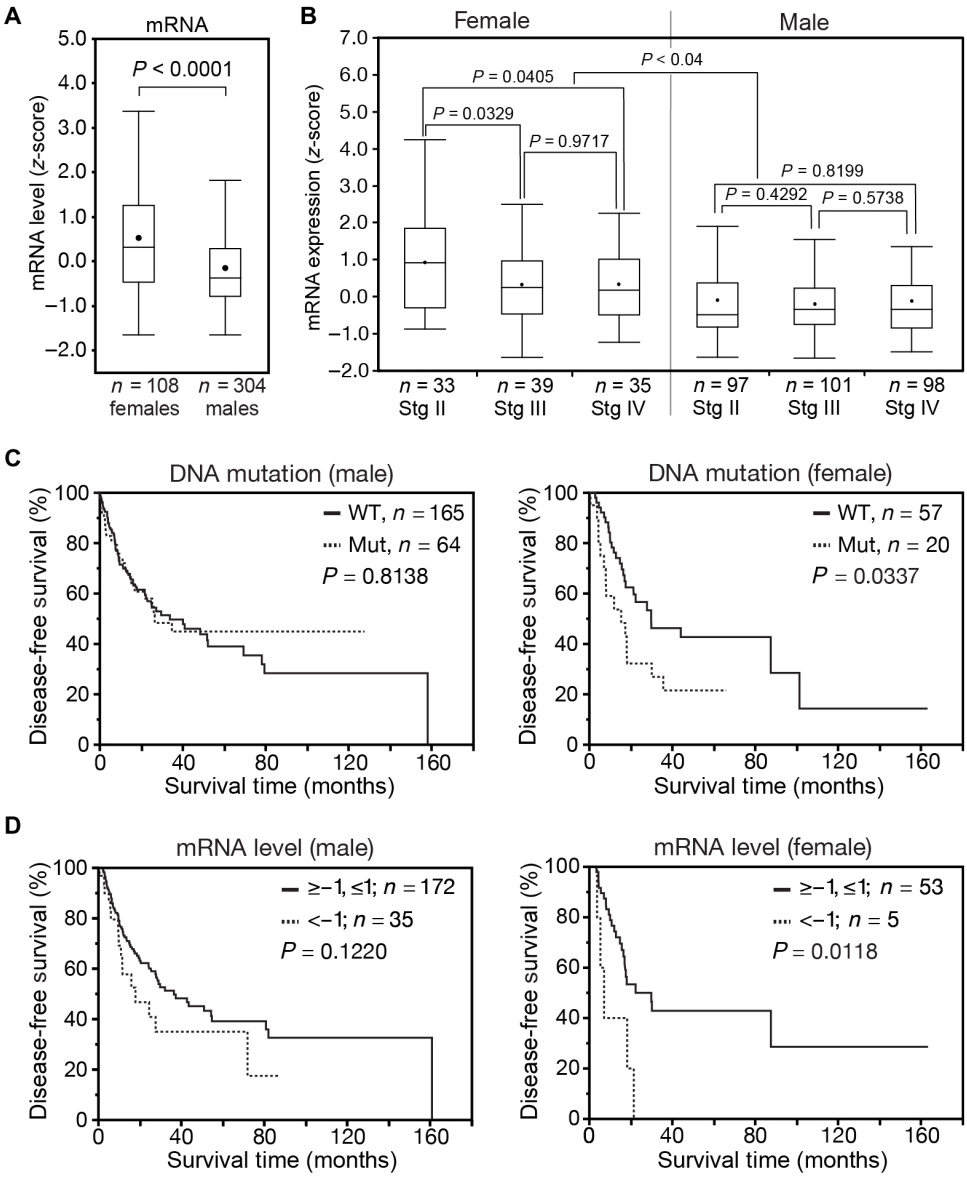

Fig. 4. Mutations and reduced expression of human *KDM6A* predict poor prognosis of female patients with BCa. (**A** and **B**) Outlier box plot of *KDM6A* gene expression in BCa samples from males and females (A) and from different cancer stages (B). Student's *t* test. (**C** and **D**) *KDM6A* mutations (C) and decreased expression (D) correlate tightly to poor disease-free survival of female but not of male patients with BCa. Kaplan-Meier analysis, log-rank test.

DISCUSSION

Collectively, this study suggests that genomic inequality causes the sex differences in cancer through the biasing effects of sex chromosomes and sex hormones (fig. S9A). Effects of sex hormones and sex chromosomes are independent of each other, and together, they further amplify the sex difference in BCa. The independent biasing effect of X chromosome is, in part, mediated by the XCI escape gene *Kdm6a* via an epigenetic mechanism that regulates the p53 signaling pathway (fig. S9). Together, we propose that effects of sex chromosomes, sex hormones, and the epigenome function independently and in combination to enhance sex differences in BCa, and *Kdm6a* is a prototypical sex-biasing tumor suppressor.

Using FCG mouse model to interrogate sex differences in cancer

Previous studies of sex differences in cancer have shown that sex hormones, particularly androgens, play a key role in the male dominance of cancer risk and mortality, including BCa (*4*, *6*, *7*), hepatocellular carcinoma (*32*, *33*), and colonic adenomas (*34*). Independent effects of genetic sex (that is, sex chromosomes) and gonadal sex (that is, sex hormones), however, could not be accurately assessed in these studies. Genetic sex is not linked to gonadal sex of FCG mice because the testis-determining gene *Sry* is "transferred" from the Y chromosome to an autosome (*15*). Using these mice, we demonstrate for the first time that sex chromosomes play an independent role in sex differences in BCa in mice. Moreover, we show that sex chromosomes and sex hormones amplify each other's sex-biasing effects. This synergism suggests that removing the effects of sex hormones, for example, gonadectomy of adult mice, also removes the effects of the sex chromosomes. Under this scenario, the impact of sex chromosomes could be overlooked and neglected. It is therefore important to examine other cancer types using the FCG mice to determine to what extent the concept of synergistic interactions between sex chromosomes and sex hormones that result in sex differences in cancer is universally applicable.

Sex chromosomes in cancer risk and mortality

Females with Turner syndrome are characterized by loss of one X chromosome. These XO patients often have dysfunctional ovaries and fail to produce sex hormones during puberty. In addition, the overall risk of solid tumors, including BCa, in patients with Turner syndrome is significantly higher compared to the general population (*35*, *36*). Conversely, males with Klinefelter syndrome, who have two or more copies of the X chromosome, display an overall reduction of the risk of solid tumors (*36*). A common clinical presentation of Klinefelter syndrome is smaller than normal testicles, which can lead to lower production of testosterone. Changes of cancer risk of these patients are often attributed to changes of sex hormone levels. By uncoupling effects of the chromosomal sex and gonadal sex, we show that genetic sex (XX and XY) has an independent biasing effect on BCa. The Y chromosome is unlikely to play a major role in sex differences in cancer because loss of Y increases cancer risk (*17*). We therefore suggest that X chromosome copy number difference is likely an intrinsic cause of sex differences in cancer; an extra copy of X confers better protection against cancer among XX individuals.

The X chromosome is rich in protein-coding and noncoding genes with diverse functions, as exemplified by the complex presentations of Turner and Klinefelter syndromes. To better understand the tumor suppressor role of the X chromosome, we have focused on the XCI escape genes because of their sexually dimorphic nature. Using RNA-seq and the FCG mice, we identified *Kdm6a* as a top candidate that is expressed in significantly higher levels in the urothelium of XX individuals. The sexually dimorphic expression pattern of *Kdm6a* correlates directly with X chromosome copy number but not gonadal type, supporting its identity as an XCI escape gene. Human *KDM6A* is often mutated in non–muscle-invasive and muscle-invasive BCas (*28*–*31*). Low *KDM6A* expression correlates tightly with BCa progression and predicts poor disease-free survival among female but not male BCa patients, consistent with the gender-specific role of *KDM6A* observed in the mice model of BCa. Clinical evidence also suggests that the sex-biasing tumor suppressor activity of *KDM6A* is limited to BCa and renal cell carcinoma. The mild effects of *KDM6A* observed in vivo and in vitro suggest that the overall protective activity of X chromosome depends on the combined effects of *KDM6A* and other X-linked tumor suppressors (*37*).

KDM6A demethylase–dependent and *KDM6A* demethylase–independent tumor suppressor activities

The demethylase activity of *KDM6A* functionally opposes PRC2 by removing the transcription-repressive mark of H3K27me3. Both wild-type and demethylase-dead *KDM6A* suppress BCa cell proliferation and anchorage-independent growth in vitro, although the mutant was less effective than the wild type. Transient expression of wild-type but not mutant *KDM6A* confers sustained repression of BCa proliferation. These findings are consistent with the observation that *KDM6A* has both demethylase-dependent and demethylase-independent activities (*24*, *25*). Moreover, our findings suggest that transient demethylase activity is sufficient for persistent suppression of tumor cell proliferation, further suggesting that loss of *KDM6A* may sensitize BCa to PRC2-dependent therapy (*38*). While statistically significant in both cases, the effect of *KDM6A* tumor suppressor in vitro is relatively mild. The underlying reason is unknown at this moment. One possible explanation is that there are additional tumor suppressors besides *KDM6A*. Alternatively, *KDM6A* activity may be limited in the cell lines used for in vitro studies, which are established from aggressive muscle-invasive BCa.

We identified *CDKN1A* and *PERP* as candidate *KDM6A* downstream effectors. We also provide evidence suggesting that *KDM6A* regulates the expression of *CDKN1A* and *PERP* in demethylase-dependent and demethylase-independent manners, respectively. Surprisingly, expression of both wild-type and mutant *KDM6A* reduces H3K27me3 at the *CDKN1A* and *PERP* loci. Since KDM6A mutant is less likely to have residual enzymatic activity (*24*), we suspect that the mutant KDM6A may recruit another demethylase such as JMJD3. Alternatively, the mutant KDM6A may indirectly regulate levels of H3K27me3 by controlling enhancer activity via the Mll3/4 complex (*25*). *CDKN1A* and *PERP* are canonical gene targets of *p53* that induce cell cycle arrest and apoptosis (*27*). Since activation of the canonical p53 gene targets may not be directly required for suppressing cancer, it remains to be determined whether and to what extent the reduced expression of *CDKN1A* and *PERP* contributed to the increased BCa risk. Nevertheless, human *KDM6A* and *p53* are co-recruited to the gene targets during embryonic stem cell differentiation and DNA damage response (*39*). In addition, genomic analyses of human fibroblasts suggest that *KDM6A* demethylase activity regulates expression of retinoblastoma (RB)–binding proteins to induce cell cycle arrest (*40*). Furthermore, we found that knockout of *Kdm6a* significantly alters the ERK/MAPK signaling pathway activity. Collectively, these observations suggest that the sexually dimorphic gene *KDM6A* may regulate tumor suppressor activities of *p53* and *RB*, as well as activities of the ERK/MAPK signaling pathway, thereby contributing to the sex differences in cancer. Findings here further suggest

that strategies of selectively targeting the *KDM6A*-dependent epigenome may blunt the sex difference in cancer by reducing cancer risk in men.

METHODS

Animals and the BBN-induced BCa model

The XYM mice (*15*) and *Kdm6a* conditional allele (*24*) were obtained from the Jackson Laboratory (stock nos. 010905 and 021926, respectively). XYM mice were generated by genetically "transferring" the sex determination gene *Sry* from the Y chromosome to chromosome 3 (*15*). Briefly, the Y-linked *Sry* gene was deleted, and the resulting mutants were XYF mice. The *Sry* transgene was subsequently reintroduced to XYF mice to generate XYM mice. Mating of XYM mice with wild-type C57Bl/6J female (XXF) mice generated an offspring with one of the four genotypes, including XXF, XXM, XYF, and XYM. The *Eed* conditional allele and *Upk2-Cre* transgenic line were reported previously (*26*). All mice were maintained on a C57Bl/6J background. The urothelium-specific *Kdm6a* and *Eed* cKO mutants were generated by crossing *Kdm6a* and *Eed* conditional alleles with *Upk2-Cre* mice. Eight-week-old mice were fed ad libitum with BBN (0.1%; TCI America) in drinking water for 14 weeks and then switched to normal water. All mice were monitored daily for death and morbidity. Mice that survived the 40-week regimen were sacrificed and considered as censored in the Kaplan-Meier survival curve analysis. All mice were examined under a stereoscope for macroscopic evidence of BCa and metastasis. All animal studies were performed according to protocols reviewed and approved by the Institutional Animal Care and Use Committee at Boston Children's Hospital.

Cell culture, doxycycline-inducible system, cell proliferation, and soft agar assays

Human urothelial carcinoma UM-UC-13 cell and mouse urothelial carcinoma MB49 cell were cultured in Dulbecco's modified Eagle's medium with 10% fetal bovine serum. *KDM6A* wild type and the catalytically dead mutant (H1146A/E1148A) were subcloned into the Gateway entry vector pEN_TTmcs and transferred subsequently to the destination vector pSLIK-Hygro and pLEX_307 using Gateway LR reaction (Invitrogen). The *KDM6a*-expression lentivirus was packed by transfection of pSLIK-*KDM6A* and pLEX-*KDM6A*, along with psPAX2 and pMD2.G to human embryonic kidney –293T cells. The inducible *KDM6A* expression lentivirus–infected UM-UC-13 cells were selected by hygromycin at 50 μg/ml. The constitutive *KDM6A* expression lentivirus–infected UM-UC-13 and MB49 cells were selected by puromycin at 5 μg/ml. To measure cell proliferation rate, cells seeded in a 96-well plate were incubated with MTT [3-(4,5-dimethylthiazol-2-yl)-2,5-diphenyltetrazolium bromide] (Invitrogen) at 0.5 mg/ml for 2 hours at 37°C. MTT metabolic product formazan was dissolved in dimethyl sulfoxide, and the optical density at 560 nm was measured, which correlated directly with cell quantity. For the soft agar assay, cells were seeded in 0.3% low–melting point agarose gel with complete growth medium that laid on 0.5% low–melting point agarose gel with complete growth medium. Colonies were stained by MTT. The colony number and size were analyzed from the captured images by ImageJ.

Plasmids, antibodies, and Western blot

KDM6A expression plasmids pCS2-*KDM6A* wild type and pCS2-*KDM6A* catalytically dead mutant (H1146A/E1148A) were gifts from K. Ge (plasmid #17438 and #40619, respectively, Addgene). Lentivirus plasmid pLEX_307 was a gift from D. Root (plasmid #41392, Addgene). Doxycycline-inducible lentivirus plasmids pSLIK-Hygro and entry plasmid pEN_TTmcs were gifts from I. Fraser (plasmid #25737 and #25755, respectively, Addgene). Lentivirus-packaging plasmids psPAX2 and pMD2.G were gifts from D. Trono (plasmid #12260 and #12259, respectively; Addgene). Anti-Myc epitope tag (71D10, Cell Signaling Technology), anti-GAPDH (SC25778, Santa Cruz Biotechnology) were used for Western blot. Anti-Histone H3K4me1, anti-Histone H3K27ac (ab4729 and ab8895, respectively; Abcam), anti-Histone H3K4me3 (39159, Active Motif), and anti-Histone H3K27me3 (07-449, Millipore) were used for ChIP. For Western blot, cells were lysed with radioimmunoprecipitation assay buffer [1% NP-40, 1% sodium deoxycholate, 20 mM tris-HCl (pH 7.6), 150 mM NaCl, 1 mM EDTA, 1 mM Na_3VO_4, 20 mM Na pyrophosphate, 20 mM β-glycerophosphate, 1 mM phenylmethylsulfonyl fluoride (PMSF), and leupeptin (1 μg/ml)]. Cell lysates were subjected to SDS–polyacrylamide gel electrophoresis and Western blot analysis.

Chromatin immunoprecipitation quantitative polymerase chain reaction

UM-UC-13 cells (one 15-cm plate at 80% confluence per ChIP) were cross-linked with 1% formalin for 10 min at room temperature and subsequently incubated with 125 mM glycine for 5 min at room temperature to quench cross-linking. Cells were washed with ice-cold phosphate-buffered saline three times and scraped off. Cells were resuspended in 20 volumes of hypotonic buffer [20 mM Hepes-KOH (pH 7.5), 10 mM KCl, 1 mM EDTA, 0.2% NP-40, 10% glycerol, 0.1 mM Na_2VO_4, 1 mM dithiothreitol, 1 mM PMSF, and 1× protease inhibitor] and incubated for 30 min on ice. Cells were homogenized 10 times by a dounce homogenizer and pelleted by centrifugation at 1000*g* for 5 min at 4°C. Nuclear pellets were lysed with lysis buffer [1% SDS, 10 mM EDTA, 50 mM tris-HCl (pH 8.1), and 1 mM PMSF] and sonicated 15 times for 20 s at 2.0 output (Misonix Sonicator 3000), allowing suspension to cool on ice for 40 s between pulses. Sonicated chromatin was cleared by centrifugation at 13,000 rpm at 4°C for 10 min. One percent of the supernatant was used as input. The supernatant was diluted 10-fold with dilution buffer [1.1% Triton X-100, 0.001% SDS, 16.7 mM tris-HCl (pH 8.1), 167 mM NaCl, and 1.2 mM EDTA] and immunoprecipitated with specific antibodies overnight at 4°C and subsequently incubated with Protein G Dynabeads (Invitrogen) at room temperature for 2 hours on a rotating platform. The beads were washed with low-salt buffer [1% Triton X-100, 0.1% SDS, 20 mM tris-HCl (pH 8.1), 150 mM NaCl, and 2 mM EDTA] once, high-salt buffer [1% Triton X-100, 0.1% SDS, 20 mM tris-HCl (pH 8.1), 500 mM NaCl, and 2 mM EDTA] once, LiCl immune complex wash buffer [1% NP-40, 1% sodium deoxycholate, 10 mM tris-HCl (pH 8.1), 250 mM LiCl, and 1 mM EDTA] once, and TE buffer [10 mM tris-HCl (pH 8.0) and 1 mM EDTA] twice. Histone/DNA complexes were eluted by incubating with elution buffer (1% SDS and 0.1 M $NaHCO_3$) at room temperature for 15 min and repeated once. The combined eluates were decross-linked by heating at 65°C for 4 hours. Decross-linked elutes were adjusted to 40 mM tris-HCl (pH 6.8), 200 mM NaCl, 10 mM EDTA, and proteinase K (0.04 μg/ml) and incubated at 45°C for 1 hour. DNA was recovered by phenol/chloroform extraction and ethanol precipitation. Enrichment was determined by qPCR using gene-specific primer sets.

Primers for ChIP-qPCR were as follows: *PERP*, TCTTAGGAGTCAGAACTGCGAC and ATACGTCAGCATGCAACCTGC (–0.9), TCAGGGGTCAGATATTAGGCTG and CTCTCCAGGCGCGTGTTTTG (–0.3), and TGTGGTGGAAATGCTCCCAAGA and CACTCACCGTACTCCATGAGG (+0.4); *CDKN1A*, GTGGCTCTGATTGGCTTTCTG and CTGAAAACAGGCAGCCCAAG (–2.2),

TGATCTGAGTTAGGTCACCAGACTTC and TCCCCACATAGCCCGTATACA (−0.9), and TTGTATATCAGGGCCGCGC and CGAATCCGCGCCCAGCTC (TSS).

RNA-seq and qRT-PCR

Bladder urothelium of FCG mice, *Kdm6a* cKO females, and littermate control females at 18 weeks were microdissected under a stereoscope. Total RNAs were isolated using TRIzol (Invitrogen) and purified by an miRNeasy kit (Qiagen) according to the manufacturer's suggested protocols. All samples with biological duplicates were sequenced using a HiSeq 4000 platform, paired-end 150 base pairs (PE150), and 40 to 70 million raw reads per sample. Paired-end clean reads were aligned to the reference genome using TopHat v2.0.9. HTSeq v0.6.1 was used to count the read numbers mapped of each gene; and RPKM (reads per kilobase of exon model per million mapped reads) of each gene was calculated on the basis of the length of the gene and read counts mapped to this gene. Differential expression analysis between two conditions/groups (two biological replicates per condition) was performed using the DESeq2 R package. *P* values were adjusted using the Benjamin-Hochberg approach for controlling the false discovery rate. Genes with $P_{adj} < 0.05$ found by DESeq2 were assigned as differentially expressed. The Venn diagrams were prepared using the function VennDiagram in R based on the gene list for different group. For qRT-PCR confirmation, total RNAs from bladder urothelium, as well as UM-UC-13 and MB49 cells, were extracted by TRIzol (Invitrogen) and purified using an RNAeasy Plus kit (Qiagen). Complementary DNA was synthesized by SuperScript III (Invitrogen). Quantitative gene expression levels were determined by qRT-PCR using gene-specific primers.

qPCR primers were as follows: human *CDKN1A*, AGGTGGACCTGGAGACTCTCAG and TCCTCTTGGAGAAGATCAGCCG; human *GAPDH*, GCCTCAAGATCATCAGCAAT and TTCAGCTCAGGGATGACCTT; human *KDM6A*, TGGAAACGTGCCTTACCTG and TGCCGAATGTGAACTCTGAC; human *PERP*, TTGTCTTCCTGAGAGTGATTGG and CCGTAGGCCCAGTTATAGATG; mouse *Cdkn1a*, CTGGTGATCTGCTGCTCTTT and CCCTGCATATACATTCCCTTCC; mouse *Gapdh*, TTGTCTCCTGCGACTTCAAC and GTCATACCAGGAAATGAGCTTG; mouse *Kdm6a*, GTGGAAGTAATGGAAACGTGC and TGTGAACTCGGACCTTTGTG; mouse *Perp*, CAGTCTAGCAACCACATCCAG and GATAAAGCCACAGAAAAGCGTG.

TCGA data analysis

TCGA data sets, including clinical and RNA-seq data, were downloaded from cBioPortal for Cancer Genomics (www.cbioportal.org) and Broad GDAC Firehose (http://gdac.broadinstitute.org). Gene expression levels were determined by RNA-seq *z*-score expression of the X chromosome genes between sexes and were analyzed using one-way analysis of variance. The association between the overall survival and gene expression levels (less than −1, low; more than +1, high; everything in between, middle) was analyzed by Kaplan-Meier analysis. Statistics, including survival (log-rank test), gene expression (one-way analysis of variance), and Cox proportional hazard model, were performed using JMP (SAS). qRT-PCR results were analyzed using Student's *t* test. $P < 0.05$ was considered significant.

SUPPLEMENTARY MATERIALS

Supplementary material for this article is available at http://advances.sciencemag.org/cgi/content/full/4/6/eaar5598/DC1

fig. S1. Schematic diagram of the BBN-induced mouse BCa model.
fig. S2. *KDM6A* functions as a demethylase-dependent and demethylase-independent tumor suppressor of BCa.
fig. S3. Schematic diagram and results of the BBN-induced BCa regimen of urothelium-specific *Kdm6a* cKO mice.
fig. S4. *KDM6A* expression levels in cancer samples are higher among female than male patients.
fig. S5. Kaplan-Meier analysis of overall survival of cancer patients stratified by *KDM6A* expression levels.
fig. S6. Candidate XCI escape genes and their mutation rates in human BCa.
fig. S7. Expression of the candidate XCI escape genes in BCa tissues from female and male patients.
fig. S8. Kaplan-Meier analysis of overall survival of cancer patients stratified by expression levels of the candidate XCI escape genes.
fig. S9. A model of molecular basis underlying the sex differences in cancer.
table S1. BCa HR of mice with different sex chromosome complement (XX versus XY) or *Kdm6a* status (wt versus mut).

REFERENCES AND NOTES

1. A. Clocchiatti, E. Cora, Y. Zhang, G. P. Dotto, Sexual dimorphism in cancer. *Nat. Rev. Cancer* **16**, 330–339 (2016).
2. G. Edgren, L. Liang, H.-O. Adami, E. T. Chang, Enigmatic sex disparities in cancer incidence. *Eur. J. Epidemiol.* **27**, 187–196 (2012).
3. P. Hartge, E. B. Harvey, W. M. Linehan, D. T. Silverman, J. W. Sullivan, R. N. Hoover, J. F. Fraumeni, Unexplained excess risk of bladder cancer in men. *J. Natl. Cancer Inst.* **82**, 1636–1640 (1990).
4. J. S. Bertram, A. W. Craig, Specific induction of bladder cancer in mice by butyl-(4-hydroxybutyl)-nitrosamine and the effects of hormonal modifications on the sex difference in response. *Eur. J. Cancer* **8**, 587–594 (1972).
5. Z. He, W. Kosinska, Z.-L. Zhao, X.-R. Wu, J. B. Guttenplan, Tissue-specific mutagenesis by N-butyl-N-(4-hydroxybutyl)nitrosamine as the basis for urothelial carcinogenesis. *Mutat. Res. Genet. Toxicol. Environ. Mutagen.* **742**, 92–95 (2012).
6. H. Miyamoto, Z. Yang, Y.-T. Chen, H. Ishiguro, H. Uemura, Y. Kubota, Y. Nagashima, Y.-J. Chang, Y.-C. Hu, M.-Y. Tsai, S. Yeh, E. M. Messing, C. Chang, Promotion of bladder cancer development and progression by androgen receptor signals. *J. Natl. Cancer Inst.* **99**, 558–568 (2007).
7. J.-W. Hsu, I. Hsu, D. Xu, H. Miyamoto, L. Liang, X.-R. Wu, C.-R. Shyr, C. Chang, Decreased tumorigenesis and mortality from bladder cancer in mice lacking urothelial androgen receptor. *Am. J. Pathol.* **182**, 1811–1820 (2013).
8. K. Shin, A. Lim, J. I. Odegaard, J. D. Honeycutt, S. Kawano, M. H. Hsieh, P. A. Beachy, Cellular origin of bladder neoplasia and tissue dynamics of its progression to invasive carcinoma. *Nat. Cell Biol.* **16**, 469–478 (2014).
9. J. Van Batavia, T. Yamany, A. Molotkov, H. Dan, M. Mansukhani, E. Batourina, K. Schneider, D. Oyon, M. Dunlop, X.-R. Wu, C. Cordon-Cardo, Cathy Mendelsohn, Bladder cancers arise from distinct urothelial sub-populations. *Nat. Cell Biol.* **16**, 982–991 (2014).
10. A. P. Arnold, A general theory of sexual differentiation. *J. Neurosci. Res.* **95**, 291–300 (2017).
11. B. P. Balaton, A. M. Cotton, C. J. Brown, Derivation of consensus inactivation status for X-linked genes from genome-wide studies. *Biol. Sex Differ.* **6**, 35 (2015).
12. J. B. Berletch, W. Ma, F. Yang, J. Shendure, W. S. Noble, C. M. Disteche, X. Deng, Escape from X inactivation varies in mouse tissues. *PLOS Genet.* **11**, e1005079 (2015).
13. T. Tukiainen, A. C. Villani, A. Yen, M. A. Rivas, J. L. Marshall, R. Satija, M. Aguirre, L. Gauthier, M. Fleharty, A. Kirby, B. B. Cummings, S. E. Castel, K. J. Karczewski, F. Aguet, A. Byrnes; GTEx Consortium, T. Lappalainen, A. Regev, K. G. Ardlie, N. Hacohen, D. G. MacArthur, Landscape of X chromosome inactivation across human tissues. *Nature* **550**, 244–248 (2017).
14. A. P. Arnold, Conceptual frameworks and mouse models for studying sex differences in physiology and disease: Why compensation changes the game. *Exp. Neurol.* **259**, 2–9 (2014).
15. P. S. Burgoyne, A. P. Arnold, A primer on the use of mouse models for identifying direct sex chromosome effects that cause sex differences in non-gonadal tissues. *Biol. Sex Differ.* **7**, 68 (2016).
16. I. Fadl-Elmula, L. Gorunova, N. Mandahl, P. Elfving, R. Lundgren, F. Mitelman, S. Heim, Karyotypic characterization of urinary bladder transitional cell carcinomas. *Genes Chromosomes Cancer* **29**, 256–265 (2000).
17. L. A. Forsberg, C. Rasi, N. Malmqvist, H. Davies, S. Pasupulati, G. Pakalapati, J. Sandgren, T. Diaz de Ståhl, A. Zaghlool, V. Giedraitis, L. Lannfelt, J. Score, N. C. P. Cross, D. Absher, E. T. Janson, C. M. Lindgren, A. P. Morris, E. Ingelsson, L. Lind, J. P. Dumanski, Mosaic loss of chromosome Y in peripheral blood is associated with shorter survival and higher risk of cancer. *Nat. Genet.* **46**, 624–628 (2014).
18. J.-H. Kim, A. Sharma, S. S. Dhar, S.-H. Lee, B. Gu, C.-H. Chan, H.-K. Lin, M. G. Lee, UTX and MLL4 coordinately regulate transcriptional programs for cell proliferation and invasiveness in breast cancer cells. *Cancer Res.* **74**, 1705–1717 (2014).

19. A. Benyoucef, C. G. Palii, C. Wang, C. J. Porter, A. Chu, F. Dai, V. Tremblay, P. Rakopoulos, K. Singh, S. Huang, F. Pflumio, J. Hébert, J.-F. Couture, T. J. Perkins, K. Ge, F. J. Dilworth, M. Brand, UTX inhibition as selective epigenetic therapy against TAL1-driven T-cell acute lymphoblastic leukemia. *Genes Dev.* **30**, 508–521 (2016).
20. J. Van der Meulen, V. Sanghvi, K. Mavrakis, K. Durinck, F. Fang, F. Matthijssens, P. Rondou, M. Rosen, T. Pieters, P. Vandenberghe, E. Delabesse, T. Lammens, B. De Moerloose, B. Menten, N. Van Roy, B. Verhasselt, B. Poppe, Y. Benoit, T. Taghon, A. M. Melnick, F. Speleman, H.-G. Wendel, P. Van Vlierberghe, The H3K27me3 demethylase UTX is a gender-specific tumor suppressor in T-cell acute lymphoblastic leukemia. *Blood* **125**, 13–21 (2015).
21. P. Ntziachristos, A. Tsirigos, G. G. Welstead, T. Trimarchi, S. Bakogianni, L. Xu, E. Loizou, L. Holmfeldt, A. Strikoudis, B. King, J. Mullenders, J. Becksfort, J. Nedjic, E. Paietta, M. S. Tallman, J. M. Rowe, G. Tonon, T. Satoh, L. Kruidenier, R. Prinjha, S. Akira, P. Van Vlierberghe, A. A. Ferrando, R. Jaenisch, C. G. Mullighan, I. Aifantis, Contrasting roles of histone 3 lysine 27 demethylases in acute lymphoblastic leukaemia. *Nature* **514**, 513–517 (2014).
22. M. L. Nickerson, N. Witte, K. M. Im, S. Turan, C. Owens, K. Misner, S. X. Tsang, Z. Cai, S. Wu, M. Dean, J. C. Costello, D. Theodorescu, Molecular analysis of urothelial cancer cell lines for modeling tumor biology and drug response. *Oncogene* **36**, 35–46 (2017).
23. M. T. Cheah, J. Y. Chen, D. Sahoo, H. Contreras-Trujillo, A. K. Volkmer, F. A. Scheeren, J. P. Volkmer, I. L. Weissman, CD14-expressing cancer cells establish the inflammatory and proliferative tumor microenvironment in bladder cancer. *Proc. Natl. Acad. Sci. U.S.A.* **112**, 4725–4730 (2015).
24. C. Wang, J. E. Lee, Y. W. Cho, Y. Xiao, Q. Jin, C. Liu, K. Ge, UTX regulates mesoderm differentiation of embryonic stem cells independent of H3K27 demethylase activity. *Proc. Natl. Acad. Sci. U.S.A.* **109**, 15324–15329 (2012).
25. H. Faralli, C. Wang, K. Nakka, A. Benyoucef, S. Sebastian, L. Zhuang, A. Chu, C. G. Palii, C. Liu, B. Camellato, M. Brand, K. Ge, F. J. Dilworth, UTX demethylase activity is required for satellite cell-mediated muscle regeneration. *J. Clin. Invest.* **126**, 1555–1565 (2016).
26. C. Guo, Z. R. Balsara, W. G. Hill, X. Li, Stage- and subunit-specific functions of polycomb repressive complex 2 in bladder urothelial formation and regeneration. *Development* **144**, 400–408 (2017).
27. M. Fischer, Census and evaluation of p53 target genes. *Oncogene* **36**, 3943–3956 (2017).
28. J. Hedegaard, P. Lamy, I. Nordentoft, F. Algaba, S. Høyer, B. P. Ulhøi, S. Vang, T. Reinert, G. G. Hermann, K. Mogensen, M. B. H. Thomsen, M. M. Nielsen, M. Marquez, U. Segersten, M. Aine, M. Höglund, K. Birkenkamp-Demtröder, N. Fristrup, M. Borre, A. Hartmann, R. Stöhr, S. Wach, B. Keck, A. K. Seitz, R. Nawroth, T. Maurer, C. Tulic, T. Simic, K. Junker, M. Horstmann, N. Harving, A. C. Petersen, M. L. Calle, E. W. Steyerberg, W. Beukers, K. E. M. van Kessel, J. B. Jensen, J. S. Pedersen, P. U. Malmström, N. Malats, F. X. Real, E. C. Zwarthoff, T. F. Ørntoft, L. Dyrskjøt, Comprehensive transcriptional analysis of early-stage urothelial carcinoma. *Cancer Cell* **30**, 27–42 (2016).
29. Cancer Genome Atlas Research Network, Comprehensive molecular characterization of urothelial bladder carcinoma. *Nature* **507**, 315–322 (2014).
30. A. G. Robertson, J. Kim, H. Al-Ahmadie, J. Bellmunt, G. Guo, A. D. Cherniack, T. Hinoue, P. W. Laird, K. A. Hoadley, R. Akbani, M. A. A. Castro, E. A. Gibb, R. S. Kanchi, D. A. Gordenin, S. A. Shukla, F. Sanchez-Vega, D. E. Hansel, B. A. Czerniak, V. E. Reuter, X. Su, B. de Sa Carvalho, V. S. Chagas, K. L. Mungall, S. Sadeghi, C. S. Pedamallu, Y. Lu, L. J. Klimczak, J. Zhang, C. Choo, A. I. Ojesina, S. Bullman, K. M. Leraas, T. M. Lichtenberg, C. J. Wu, N. Schultz, G. Getz, M. Meyerson, G. B. Mills, D. J. McConkey; TCGA Research Network, J. N. Weinstein, D. J. Kwiatkowski, S. P. Lerner, Comprehensive molecular characterization of muscle-invasive bladder cancer. *Cell* **171**, 540–556.e25 (2017).
31. Y. Gui, G. Guo, Y. Huang, X. Hu, A. Tang, S. Gao, R. Wu, C. Chen, X. Li, L. Zhou, M. He, Z. Li, X. Sun, W. Jia, J. Chen, S. Yang, F. Zhou, X. Zhao, S. Wan, R. Ye, C. Liang, Z. Liu, P. Huang, C. Liu, H. Jiang, Y. Wang, H. Zheng, L. Sun, X. Liu, Z. Jiang, D. Feng, J. Chen, S. Wu, J. Zou, Z. Zhang, R. Yang, J. Zhao, C. Xu, W. Yin, Z. Guan, J. Ye, H. Zhang, J. Li, K. Kristiansen, M. L. Nickerson, D. Theodorescu, Y. Li, X. Zhang, S. Li, J. Wang, H. Yang, J. Wang, Z. Cai, Frequent mutations of chromatin remodeling genes in transitional cell carcinoma of the bladder. *Nat. Genet.* **43**, 875–878 (2011).
32. Z. Li, G. Tuteja, J. Schug, K. H. Kaestner, Foxa1 and Foxa2 are essential for sexual dimorphism in liver cancer. *Cell* **148**, 72–83 (2012).
33. W. E. Naugler, T. Sakurai, S. Kim, S. Maeda, K. Kim, A. M. Elsharkawy, M. Karin, Gender disparity in liver cancer due to sex differences in MyD88-dependent IL-6 production. *Science* **317**, 121–124 (2007).
34. J. M. Amos-Landgraf, J. Heijmans, M. C. B. Wielenga, E. Dunkin, K. J. Krentz, L. Clipson, A. G. Ederveen, P. G. Groothuis, S. Mosselman, V. Muncan, D. W. Hommes, A. Shedlovsky, W. F. Dove, G. R. van den Brink, Sex disparity in colonic adenomagenesis involves promotion by male hormones, not protection by female hormones. *Proc. Natl. Acad. Sci. U.S.A.* **111**, 16514–16519 (2014).
35. M. J. Schoemaker, A. J. Swerdlow, C. D. Higgins, A. F. Wright, P. A. Jacobs; UK Clinical Cytogenetics Group, Cancer incidence in women with Turner syndrome in Great Britain: A national cohort study. *Lancet Oncol.* **9**, 239–246 (2008).
36. J. Ji, B. Zöller, J. Sundquist, K. Sundquist, Risk of solid tumors and hematological malignancy in persons with Turner and Klinefelter syndromes: A national cohort study. *Int. J. Cancer* **139**, 754–758 (2016).
37. A. Dunford, D. M. Weinstock, V. Savova, S. E. Schumacher, J. P. Cleary, A. Yoda, T. J. Sullivan, J. M. Hess, A. A. Gimelbrant, R. Beroukhim, M. S. Lawrence, G. Getz, A. A. Lane, Tumor-suppressor genes that escape from X-inactivation contribute to cancer sex bias. *Nat. Genet.* **49**, 10–16 (2017).
38. L. D. Ler, S. Ghosh, X. Chai, A. A. Thike, H. L. Heng, E. Y. Siew, S. Dey, L. K. Koh, J. Q. Lim, W. K. Lim, S. S. Myint, J. L. Loh, P. Ong, X. X. Sam, D. Huang, T. Lim, P. H. Tan, S. Nagarajan, C. W. S. Cheng, H. Ho, L. G. Ng, J. Yuen, P.-H. Lin, C.-K. Chuang, Y.-H. Chang, W.-H. Weng, S. G. Rozen, P. Tan, C. L. Creasy, S.-T. Pang, M. T. McCabe, S. L. Poon, B. T. Teh, Loss of tumor suppressor KDM6A amplifies PRC2-regulated transcriptional repression in bladder cancer and can be targeted through inhibition of EZH2. *Sci. Transl. Med.* **9**, aai8312 (2017).
39. K. C. Akdemir, A. K. Jain, K. Allton, B. Aronow, X. Xu, A. J. Cooney, W. Li, M. C. Barton, Genome-wide profiling reveals stimulus-specific functions of p53 during differentiation and DNA damage of human embryonic stem cells. *Nucleic Acids Res.* **42**, 205–223 (2014).
40. J. K. Wang, M.-C. Tsai, G. Poulin, A. S. Adler, S. Chen, H. Liu, Y. Shi, H. Y. Chang, The histone demethylase UTX enables RB-dependent cell fate control. *Genes Dev.* **24**, 327–332 (2010).

Acknowledgments: We thank X. Shi, C. Guo, and J. Lin for the technical assistance; R. Adam, K. Li, K. Liang, and M. Zhang for the critical reading of the manuscript; and Y. Sun, C. Nelson, Z. Li, X. Sun, M. Kurtz, and J. McQuaid for the helpful discussions. **Funding:** This work was supported by the NIH/National Cancer Institute (1R21CA198544 to X.L.). **Author contributions:** X.L. conceived the ideas and designed the experiments. S.K. performed and designed the experiments and analyzed the TCGA data sets. **Competing interests:** The authors declare that they have no competing interests. **Data and materials availability:** All data needed to evaluate the conclusions in the paper are present in the paper and/or the Supplementary Materials. Additional data related to this paper may be requested from the authors. Correspondence and requests for materials should be addressed to X.L. (sean.li@childrens.harvard.edu).

Submitted 21 November 2017
Accepted 27 April 2018
Published 13 June 2018
10.1126/sciadv.aar5598

Citation: S. Kaneko, X. Li, X chromosome protects against bladder cancer in females via a *KDM6A*-dependent epigenetic mechanism. *Sci. Adv.* **4**, eaar5598 (2018).